FOXP3+ Tregs require WASP to restrain Th2-mediated food allergy

Willem S. Lexmond,[1,2] Jeremy A. Goettel,[1,2] Jonathan J. Lyons,[3] Justin Jacobse,[1] Marion M. Deken,[1] Monica G. Lawrence,[4] Thomas H. DiMaggio,[3] Daniel Kotlarz,[1,5] Elizabeth Garabedian,[6] Paul Sackstein,[3] Celeste C. Nelson,[3] Nina Jones,[7] Kelly D. Stone,[8] Fabio Candotti,[9] Edmond H.H.M. Rings,[10] Adrian J. Thrasher,[11] Joshua D. Milner,[3] Scott B. Snapper,[1,2,12] and Edda Fiebiger[1,2]

[1]Department of Pediatrics, Division of Gastroenterology, Hepatology and Nutrition, Boston Children's Hospital, Boston, Massachusetts, USA. [2]Department of Medicine, Harvard Medical School, Boston, Massachusetts, USA. [3]Genetics and Pathogenesis of Allergy Section, Laboratory of Allergic Diseases, National Institute of Allergy and Infectious Diseases (NIAID), NIH, Bethesda, Maryland, USA. [4]Division of Asthma, Allergy and Immunology, Department of Medicine, University of Virginia Health System, Charlottesville, Virginia, USA. [5]Department of Pediatrics, Dr. von Hauner Children's Hospital, Ludwig-Maximilians-University, Munich, Germany. [6]National Human Genome Research Institute, NIH, Bethesda, Maryland, USA. [7]Clinical Research Directorate/Clinical Monitoring Research Program (CMRP), Leidos Biomedical Research Inc., National Cancer Institute (NCI) Campus at Frederick, Frederick, Maryland, USA. [8]Laboratory of Allergic Diseases, NIAID, NIH, Bethesda, Maryland, USA. [9]Genetics and Molecular Biology Branch, National Human Genome Research Institute (NHGRI), NIH, Bethesda, Maryland, USA. [10]Departments of Pediatrics, Erasmus University, Erasmus Medical Center, Rotterdam and Leiden University, University Medical Center Leiden, Leiden, Netherlands. [11]Great Ormond Street Hospital NHS Trust, London and Institute of Child Health, University College London, London, United Kingdom. [12]Division of Gastroenterology, Department of Medicine, Brigham and Women's Hospital, Boston, Massachusetts, USA.

In addition to the infectious consequences of immunodeficiency, patients with Wiskott-Aldrich syndrome (WAS) often suffer from poorly understood exaggerated immune responses that result in autoimmunity and elevated levels of serum IgE. Here, we have shown that WAS patients and mice deficient in WAS protein (WASP) frequently develop IgE-mediated reactions to common food allergens. WASP-deficient animals displayed an adjuvant-free IgE-sensitization to chow antigens that was most pronounced for wheat and soy and occurred under specific pathogen–free as well as germ-free housing conditions. Conditional deletion of Was in FOXP3+ Tregs resulted in more severe Th2-type intestinal inflammation than that observed in mice with global WASP deficiency, indicating that allergic responses to food allergens are dependent upon loss of WASP expression in this immune compartment. While WASP-deficient Tregs efficiently contained Th1- and Th17-type effector differentiation in vivo, they failed to restrain Th2 effector responses that drive allergic intestinal inflammation. Loss of WASP was phenotypically associated with increased GATA3 expression in effector memory FOXP3+ Tregs, but not in naive-like FOXP3+ Tregs, an effect that occurred independently of increased IL-4 signaling. Our results reveal a Treg-specific role for WASP that is required for prevention of Th2 effector cell differentiation and allergic sensitization to dietary antigens.

Introduction

Type 2 immunity is involved in a variety of host-defense functions, ranging from protection against parasites and support of epithelial barrier integrity to regulation of wound healing and control of metabolic homeostasis (1–3). Many of these functions are performed by cells of the innate immune system, including eosinophils, basophils, and mast cells, which in turn are orchestrated by Th2 lymphocytes of the adaptive immune system through the production of type 2 cytokines, such as IL-4, IL-5, and IL-13. Th2 help can furthermore instruct B cells to produce IgE, which arms mast cells and basophils with antigen-specific effector functions through binding to their high-affinity IgE receptor FcεRI on the cell surface. Despite the presence of multiple inhibitory pathways of type 2 immunity (1), dysregulation within this system is increasingly common in Westernized societies and can result in the production of allergen-specific IgE, type I hypersensitivity reactions, and allergic tissue inflammation (1–3). In order to better understand the recent surge in incidence as well as the pathogenesis of Th2-driven allergic diseases, the study of aberrant activation of Th2 effector responses is of critical importance.

As is true for Th1 responses, Th2-mediated immune reactions critically rely on the function of Tregs for their containment. Functional defects in FOXP3, the lineage-defining transcription factor that identifies the best-characterized population of Tregs, result in the immune dysregulation, polyendocrinopathy, enteropathy, X-linked (IPEX) syndrome in human patients and in the IPEX-related scurfy phenotype in mice (4). In both species, the severe lymphoproliferation that ensues shows concomitant Th1 and Th2 effector responses, which may counterregulate each other (5), and manifests clinically as a loss of tolerance to self and autoimmunity in combination with elevated IgE levels and food allergies (5–7). Emerging data implicate functionally distinct subsets of CD4+FOXP3+ Tregs that exert differential control over Th1 and Th2 effector cell proliferation, which may be related to their anatomic location of origin. For instance, thymus-derived Tregs were recently shown to specifically control Th1 immunity (8), whereas

selective loss of peripherally induced Foxp3+ Tregs (iTregs) resulted in uncontrolled Th2, but not Th1- or Th17-type, inflammation (9). These findings fit within the broader paradigm that lineage-committed FOXP3+ Tregs are responsive to environmental cues and can assume tissue-specific phenotypes by coopting other transcription factors such as GATA3 or T-bet (10–12). The mechanisms and consequences of this phenotypic variation and functional plasticity are only beginning to be understood.

In addition to the human IPEX syndrome, dysregulated Th2 responses, atopy, and elevated IgE levels occur in a range of primary human immunodeficiencies, some of which are phenocopied in the corresponding mouse models (13–18). The variety of genes that are affected in these disorders — e.g., *STAT3*, *DOCK8*, *PGM3* and multiple genes involved in TCR signaling such as *LAT*, *ZAP70*, or *RAG* — suggests that hyper IgE phenotypes can result from alterations in a number of distinct immunological pathways. In most of these cases, however, the underlying mechanisms of increased IgE production or the functional consequences of elevated serum IgE (sIgE) have not been studied in detail.

One well-known primary immunodeficiency with elevated sIgE is Wiskott-Aldrich syndrome (WAS) (13, 14). WAS is caused by mutations in the *WAS* gene on the X chromosome, which encodes the WAS protein (WASP) with expression restricted to hematopoietic lineages. WASP is the founding member of a family of actin regulators, capable of transducing a variety of signals to mediate changes in the actin cytoskeleton, and has been implicated in a great variety of cellular functions in both lymphocytes and nonlymphocytes (19, 20). More than 100 unique loss-of-function mutations in *WAS* have been reported, giving rise to a clinically heterogeneous group of patients (19). The most severely affected males present early in life with thrombocytopenia, eczema, autoimmune sequelae, and recurrent infections, which can be fatal in the absence of bone marrow transplantation or gene therapy. In contrast, milder loss-of-function mutations have been identified in patients who suffer from an attenuated form of the disease termed X-linked thrombocytopenia (XLT), which has excellent long-term survival with medical management alone (21). Despite the long-known association between *WAS* mutations and atopy, the antigenic specificity of the expanded IgE pool and the consequences of elevated IgE on the prevalence of allergic disease are only beginning to be investigated in human patients (22) and have not been addressed in WASP-deficient mice.

Here, we show that patients with mutations in *WAS* demonstrate an increased frequency of sensitization to food allergens as measured by serum-specific IgE and skin-prick testing (SPT) and increased prevalence of clinically relevant food allergy in childhood when compared with the general population. Similarly, *Was*−/− mice spontaneously develop IgE-mediated immune responses and intestinal mast cell expansion. Using conditional WASP-deficient mice, we identified that WASP deficiency limited to FOXP3+ Tregs results in a strongly Th2-skewed, allergic inflammation of the small intestine, which was exacerbated compared with that of complete *Was*−/− counterparts. Phenotypically, WASP-deficient Tregs displayed elevated levels of Th2 transcription factor GATA3 in the effector-like, but not naive, subset of FOXP3+ Tregs, which occurred independently of IL-4. These findings demonstrate that WASP is required for FOXP3+ Tregs to exert selective control over Th2-type immune responses.

Results

Sensitization to food antigens and food allergy are enriched among patients with WAS mutations. We assessed the overall burden of clinical food allergy within a cohort of 25 patients with mutations in the *WAS* gene. Results from 3 patients were excluded from the analysis, as they could not be tested prior to hematopoietic stem cell transplantation (HSCT). A variety of *WAS* mutations were observed in this cohort (Figure 1A), which consisted of patients with both WAS (*n* = 15) and XLT (*n* = 10). Elevated IgE (normal range, 0–90 IU/ml) was observed in 59% of patients (13/22), and food allergen–specific IgE was detected in 33% (4/12) of WAS and 20% (2/10) of XLT patients (Figure 1B) (23). Compared with the general population, individuals with *WAS* mutations were more likely to demonstrate serum sensitization to peanut, milk, and egg (Figure 1C) (23). The prevalence of physician-diagnosed food allergy among WAS and XLT patients in childhood (20% and 30%, respectively) was also increased compared with rates reported among children in the National Health and Nutrition Examination Survey (NHANES) (6.5%) (24) and approached levels reported among children with moderate-to-severe atopic dermatitis (37% ± 13%) (Figure 1C) (25), although none of the patients reported a history of anaphylaxis. Food sensitization was generally detected with greater sensitivity using sIgE testing than by SPT (Figure 1D): peanut and egg white allergens failed to elicit positive SPT responses in 2 physician-diagnosed food allergic patients who were found positive for sIgE against these 2 allergens (Figure 1D). One patient with a clinical history consistent with food allergy was negative both by SPT and by serum-specific IgE to all tested food antigens. Five additional patients who underwent sIgE testing could not have SPT performed and were not included in evaluating the sIgE/SPT concordance rates. Patients with mutations in WAS demonstrated dampened wheal responses to skin challenge with morphine (Figure 1E), suggesting that WASP deficiency in mast cells may contribute to the high discordance of sIgE levels and SPT responses. Taken together, our data demonstrate a marked enrichment of clinically relevant food antigen–specific IgE in patients with mutations in *WAS*.

Was−/− *mice spontaneously develop IgE-mediated immune responses to food allergens.* Following the observation that WAS patients frequently develop IgE antibodies against food antigens, we investigated the occurrence of IgE-mediated responses to allergens in chow in WASP-deficient mice. *Was*−/− females or hemizygous *Was*−/ males (henceforth both referred to as *Was*−/− mice) on BALB/c, C57BL/6, and 129SvEv backgrounds developed elevated levels of total sIgE and IgG1 in comparison with background-matched WT controls (Figure 2A and Supplemental Figure 1, A and C; supplemental material available online with this article; doi:10.1172/JCI85129DS1). sIgE increased with age and correlated positively with the density of surface-bound IgE on circulating basophils, indicating that binding of IgE to its high-affinity receptor FcεRI was unperturbed in *Was*−/− animals (Supplemental Figure 1, A and B). We next developed ELISA-based assays to screen for antibodies against the 5 main components of mouse chow. Food-specific antibodies were not detected in WT mice, while soy- and wheat-specific IgE and IgG1 were readily detected in the serum of *Was*−/− mice (Figure 2B). For all investigated food extracts, a strong positive correlation between ingredient-specific titers of IgE and
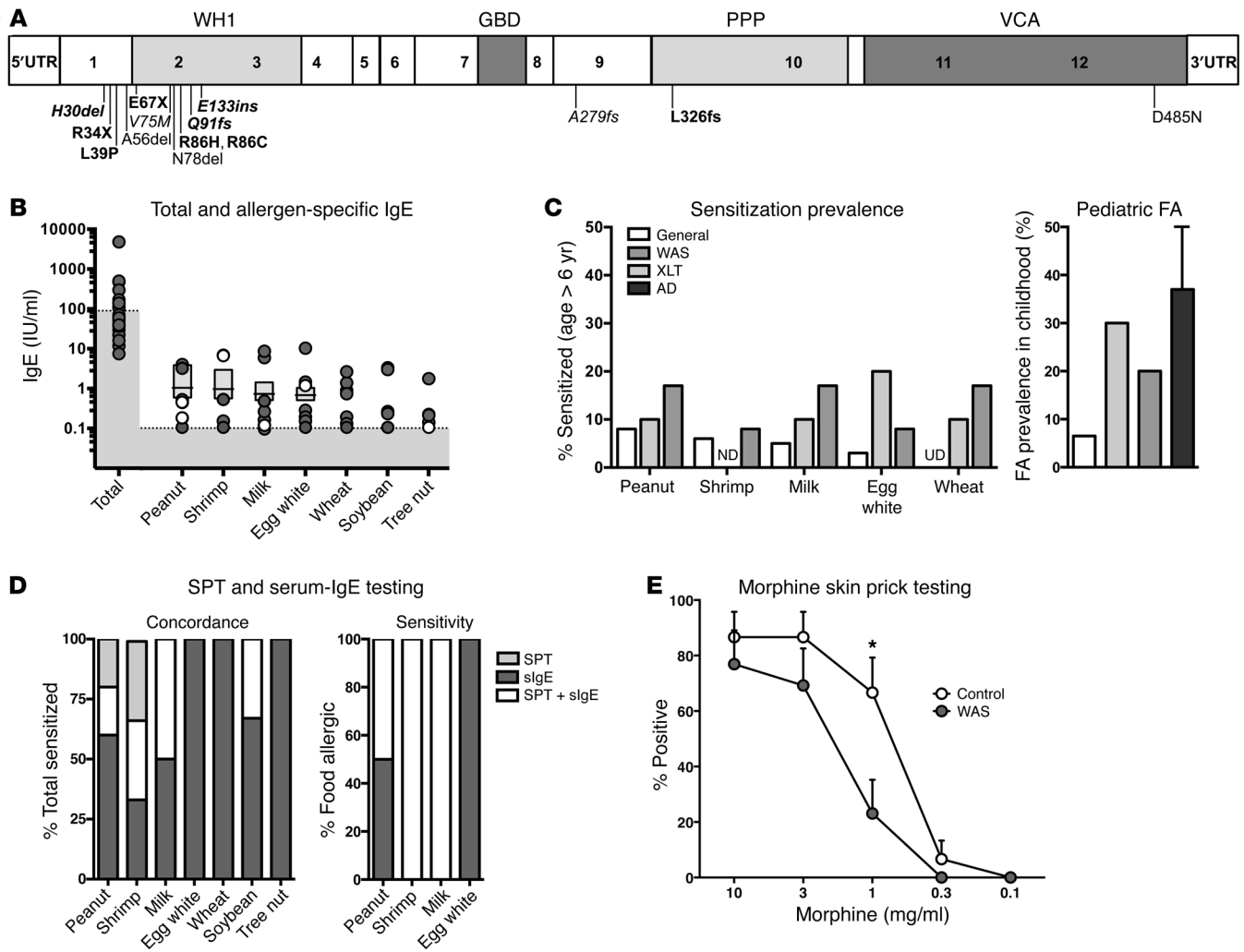
Figure 1. Increased sensitization and prevalence of food allergy among patients with *WAS* mutations. (**A**) Schematic of *WAS* gene with mutations identified among cohort (n = 25). Bold indicates WAS diagnosis; unbolded indicates XLT; italicized indicates mutations associated with food allergy in childhood. (**B**) Total serum IgE (sIgE) levels and food allergen–specific sIgE levels among cohort; limit of detection for sIgE was 0.1 IU/ml. Light gray fill indicates the normal range; boxes indicate median and interquartile ranges for 4 foods reported in NHANES (ref. 23). White circles indicate food-allergic individuals. (**C**) Among patients with sera obtained prior to transplantation (n = 22), percent of WAS (n = 12) or XLT (n = 10) patients positive for sIgE against foods (minimum cutoff 0.35 IU/ml) compared with the general population as reported in NHANES analysis (left panel). Prevalence of food allergy during childhood among all WAS (n = 15) and XLT (n = 10) patients compared with those reported in the general population (NHANES) and in patients with moderate to severe atopic dermatitis (AD) (right panel) (refs. 24 and 25). (**D**) Concordance between sIgE measurement and SPT for foods in individuals who underwent both modalities (n = 14) (left panel). Results of SPT and sIgE testing among patients with persistent clinical food allergy (n = 4); 2 individuals with food allergy in childhood without current evidence of sensitization were excluded (right panel). (**E**) Percentage of positive wheal responses to SPT with morphine titration among patients with *WAS* mutations (n = 13) compared with sex-matched controls (n = 15), *P = 0.03 by Fisher's exact test. UD, undefined; ND, none detected; WH1, WASP Homology domain 1; GBD, GTPase binding domain; PPP, polyproline domain; VCA, verprolin homology, cofilin homology, and acidic region domain.

IgG1 was observed (Supplemental Figure 1D). The observation that food-specific IgE could be detected in *Was⁻/⁻* mice on 3 different genetic backgrounds indicated that sensitization to ingested antigens did not result from colonic inflammation since, in contrast to *Was⁻/⁻* mice on the colitis-prone 129SvEv background (26, 27), animals on the BALB/c and C57BL/6 background are resistant to colitis (Supplemental Figure 1, E and F).

To assess whether food-specific sIgE from *Was⁻/⁻* mice was functional in mediating type I hypersensitivity reactions, bone marrow–derived WT mast cells were loaded with serum from *Was⁻/⁻* mice previously identified by ELISA to be sensitized to food antigens or with serum from *Was⁻/⁻* mice of comparable IgE titer

that had been found to not be sensitized to food (Figure 2C). The appearance of lysosomal-associated membrane protein 1 (LAMP-1) at the cell surface of mast cells is an established surrogate marker for antigen/IgE-mediated histamine release (28, 29), and we found that WT mast cells loaded with serum from food-sensitized *Was⁻/⁻* mice degranulated in response to stimulation with an antigen extract from conventional chow, but not in response to an extract from a protein-free, amino acid–based elemental diet (Figure 2C). In contrast, mast cells loaded with serum from non–food-sensitized animals were not activated by either food extract, which further demonstrated that IgE-dependent degranulation was antigen specific and established that screening of antibody
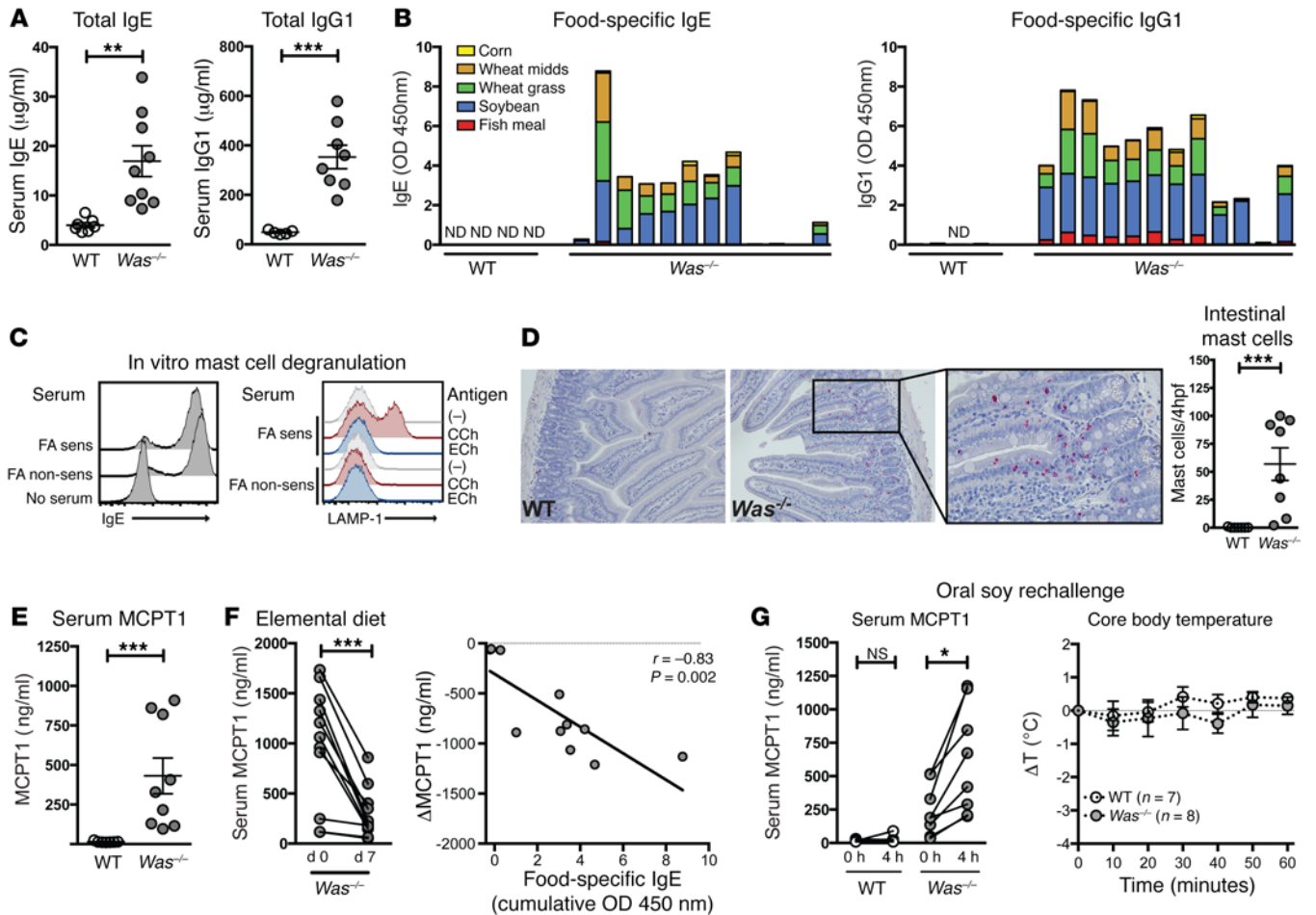
Figure 2. Spontaneous sensitization to food antigens and food allergy in *Was⁻/⁻* mice. (**A**) Comparative analysis of total sIgE and IgG1 levels in 3-month-old WT BALB/c (open circles, $n = 7$) and *Was⁻/⁻* mice (gray circles, $n = 9$) of mixed genders. (**B**) IgE and IgG1 reactivity against the 5 main (% w/w) chow components as determined by ELISA in 1:30 (IgE) or 1:1,000 (IgG1) diluted serum samples. (**C**) Loading of WT bone marrow–derived mast cells with serum of food-allergic (FA sens) or non–food-allergic (FA non-sens) *Was⁻/⁻* mice compared with no-serum control (left panel). Appearance of surface LAMP-1 as a marker of mast cell degranulation after stimulation with antigen extracts from conventional chow (CCh), elemental chow (ECh), or PBS (–). (**D**) Intestinal mast cell expansion as determined by chloroacetate esterase staining of jejunal cross-sections (×20, with digital magnification to ×50 shown in window) and quantification per 4 high-power fields (4hpf) in WT ($n = 7$) and *Was⁻/⁻* mice ($n = 8$). (**E**) Serum levels of mast cell protease 1 (MCPT1) determined by ELISA. (**F**) Effect of 7-day treatment with elemental diet on serum MCPT1 in *Was⁻/⁻* mice ($n = 11$). Spearman's rank correlation between cumulative anti-food IgE titers of mice and response to allergen elimination defined as ΔMCPT1. (**G**) Effect of oral rechallenge with 12.5 mg soy protein extract on body temperature and serum MCPT1 after 4 hours. Symbols represent individual mice and error bars depict SEM. *$P < 0.05$, **$P < 0.01$, ***$P < 0.001$ as determined by 2-tailed Student's t test. NS, not significant; ND, not detectable. Results in **C** are representative of 2 independent experiments. Equivalent results were obtained in a cohort of WT and *Was⁻/⁻* mice on the 129SvEv background.

reactivity against the 5 main chow components is a reliable marker for the overall anti-food IgE reactivity.

Expansion of intestinal mast cells is a common symptom in food-allergic patients (30, 31) and has been demonstrated to correlate with disease severity in experimental mouse models of food allergy (32–34). In line with these findings, we observed expansion of the small intestinal mast cell pool in *Was⁻/⁻* mice as detected by chloroacetate esterase staining on jejunal tissue sections (Figure 2D). In addition, mRNA expression levels of the mucosal mast cell marker mast cell protease 1 (*Mcpt1*) were elevated in *Was⁻/⁻* animals and positively correlated with the cumulative anti-food IgE titer (Supplemental Figure 1G). Since *Was⁻/⁻* mice cannot eliminate food antigens from their diet, we hypothesized that persistent oral allergen exposure would result in continuous IgE/FcεRI-mediat-

ed degranulation of intestinal mast cells. Indeed, *Was⁻/⁻* animals had elevated serum levels of the mast cell protease MCPT1 (Figure 2E), which is released from mucosal mast cells in response to IgE-mediated detection of food antigens (32, 35). Moreover, anti-food IgE titers positively correlated with serum MCPT1 levels (Supplemental Figure 1H). Consistent with a critical role for food antigens in mast cell activation, elimination of the dietary allergens via switching *Was⁻/⁻* mice from conventional chow to an elemental amino acid–based chow resulted in a decline in serum MCPT1 after 7 days, with the most pronounced therapeutic effect (defined as ΔMCPT1) observed in mice with the highest cumulative anti-food IgE titers (Figure 2F). Oral rechallenge with soy extract after more than a week of allergen elimination led to rapid activation of mucosal mast cells indicated by increased levels of serum MCPT1,
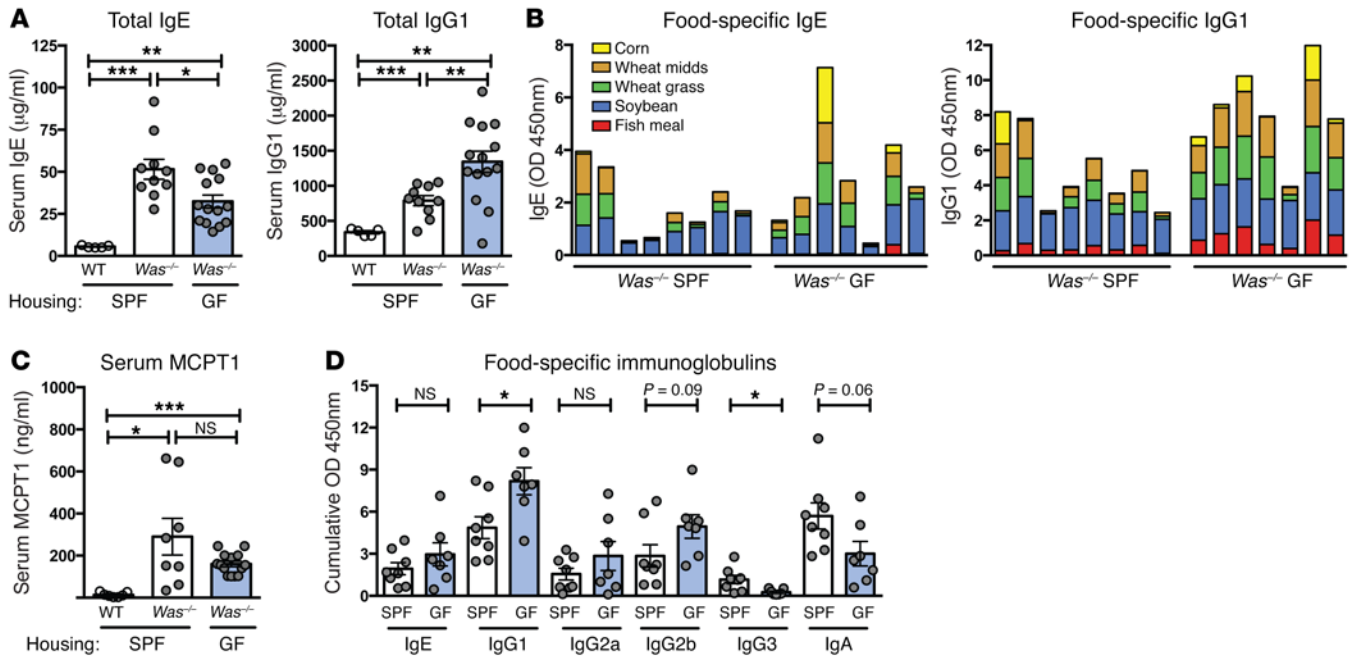
Figure 3. Commensals are dispensable for spontaneous sensitization to food in *Was⁻/⁻* mice but shape the isotype composition of the humoral anti-food response. (**A**) Comparison of total IgE and total IgG1 serum levels in 4- to 6-month-old WT (open circles, n = 5) or *Was⁻/⁻* (gray circles) on the 129SvEv background that were housed under either SPF (n = 10) or GF (n = 14) conditions. (**B**) Food-specific IgE and IgG1 for the 5 main chow constituents in IgE (serum dilution 1:100) or IgG1 (1:5,000) from SPF (n = 8) and GF (n = 7) *Was⁻/⁻* mice. (**C**) Comparison of serum MCPT1 levels. (**D**) Comparison of cumulative anti-food titers of IgE, IgG1, IgG2a (1:1,000), IgG2b (1:1,000), IgG3 (1:200), and IgA (1:5,000) in SPF (n = 8) and GF (n = 7) *Was⁻/⁻* animals. Symbols represent individual mice and error bars depict SEM. *P < 0.05, **P < 0.01, ***P < 0.001. NS, not significant as determined by 2-tailed Student's t test. Results are shown from sera obtained from mice from ≥ 3 independent cohorts.

but did not result in signs of anaphylactic shock as measured by a reduction in core body temperature (Figure 2G). Combined, these data demonstrate that *Was⁻/⁻* mice develop food-specific IgE, which effectively mediates mast cell degranulation in vitro and in vivo.

The microbial flora is dispensable for spontaneous oral sensitization to chow, but shapes the humoral anti-food response in Was⁻/⁻ mice. Since commensal microbes play a dominant role in regulating IgE-mediated responses to food antigens (36–38), we assessed the contribution of the microbiome to the induction of food-specific IgE responses in *Was⁻/⁻* animals. When compared with specific pathogen–free–housed (SPF-housed) WT mice, both SPF and germ-free (GF) *Was⁻/⁻* mice showed elevated total IgE and IgG1 levels. Although total IgE was lower in GF *Was⁻/⁻* than in SPF *Was⁻/⁻* animals (Figure 3A), detailed food-specificity profiling of IgE and IgG1 revealed that sensitization to food occurred efficiently in mice housed under either condition (Figure 3B), with MCPT1 titers comparable between SPF and GF *Was⁻/⁻* mice (Figure 3C). Further comparative analysis of the isotype composition of the humoral anti-food response in GF *Was⁻/⁻* and SPF *Was⁻/⁻* mice showed that anti-food IgG1 and IgG2b titers were elevated in the absence of microbes, whereas food-specific IgG3 and IgA levels were diminished (Figure 3D and Supplemental Figure 2). Since the chow used in the SPF and GF settings differed only by 1 additional cycle of high-dose irradiation in the latter, it is reasonable to assume that all *Was⁻/⁻* animals were exposed to food of nearly identical antigenicity. Consequently, food-specific IgE responses in *Was⁻/⁻* mice do not require microbial modifications or cosignals that could potentially confer allergenic properties to food antigens. Moreover,

these results demonstrate that food allergy in *Was⁻/⁻* animals does not require alterations in the commensal flora that may possibly occur as a consequence of WASP deficiency.

Conditional deletion of WASP in FOXP3⁺ Tregs results in exacerbated Th2-type intestinal inflammation. WASP is expressed in all hematopoietic lineages, and its deficiency in dendritic cells, B cells, effector T cells, or Tregs has been described as having a variety of consequences for immune responses (19, 27, 39, 40). Unlike *Was⁻/⁻* mice, *Was⁻/⁻Rag2⁻/⁻* double-knockout mice presented with serum MCPT1 levels comparable to WT or *Rag2⁻/⁻* animals (Supplemental Figure 3A), indicating that intestinal mast cell expansion and activation in WASP deficiency do not occur in the absence of an adaptive immune system. We next analyzed strains with conditional deletion of WASP in B cells *(Wasᶠˡ/ᶠˡ Mb1-Cre)*, CD11c⁺ dendritic cells *(Wasᶠˡ/ᶠˡ Itgax-Cre)*, or FOXP3⁺ Tregs *(Wasᶠˡ/ᶠˡ Foxp3-Cre)*. Elevated serum MCPT1 was not found in animals harboring conditional deletions of WASP in B cells or dendritic cells, but was present in *Wasᶠˡ/ᶠˡ Foxp3-Cre* females or *Wasᶠˡ/ᶠˡ Foxp3-Cre* males (henceforth also referred to as *Wasᶠˡ/ᶠˡ Foxp3-Cre* mice) on both the C57BL/6 and 129SvEv backgrounds (Figure 4A). Histological analysis confirmed a profound expansion of mucosal mast cells in the small intestine of *Wasᶠˡ/ᶠˡ Foxp3-Cre* mice but not in their *Wasᶠˡ/ᶠˡ Foxp3-Cre* littermates (Figure 4B). Mucosal mast cell infiltration occurred in the absence of gross histological changes, and we observed no evidence of colitis in *Wasᶠˡ/ᶠˡ Foxp3-Cre* mice on the C57BL/6 background (Figure 4B).

Following the observation that Treg-specific WASP deletion was sufficient for expansion of intestinal mast cells, we next asked
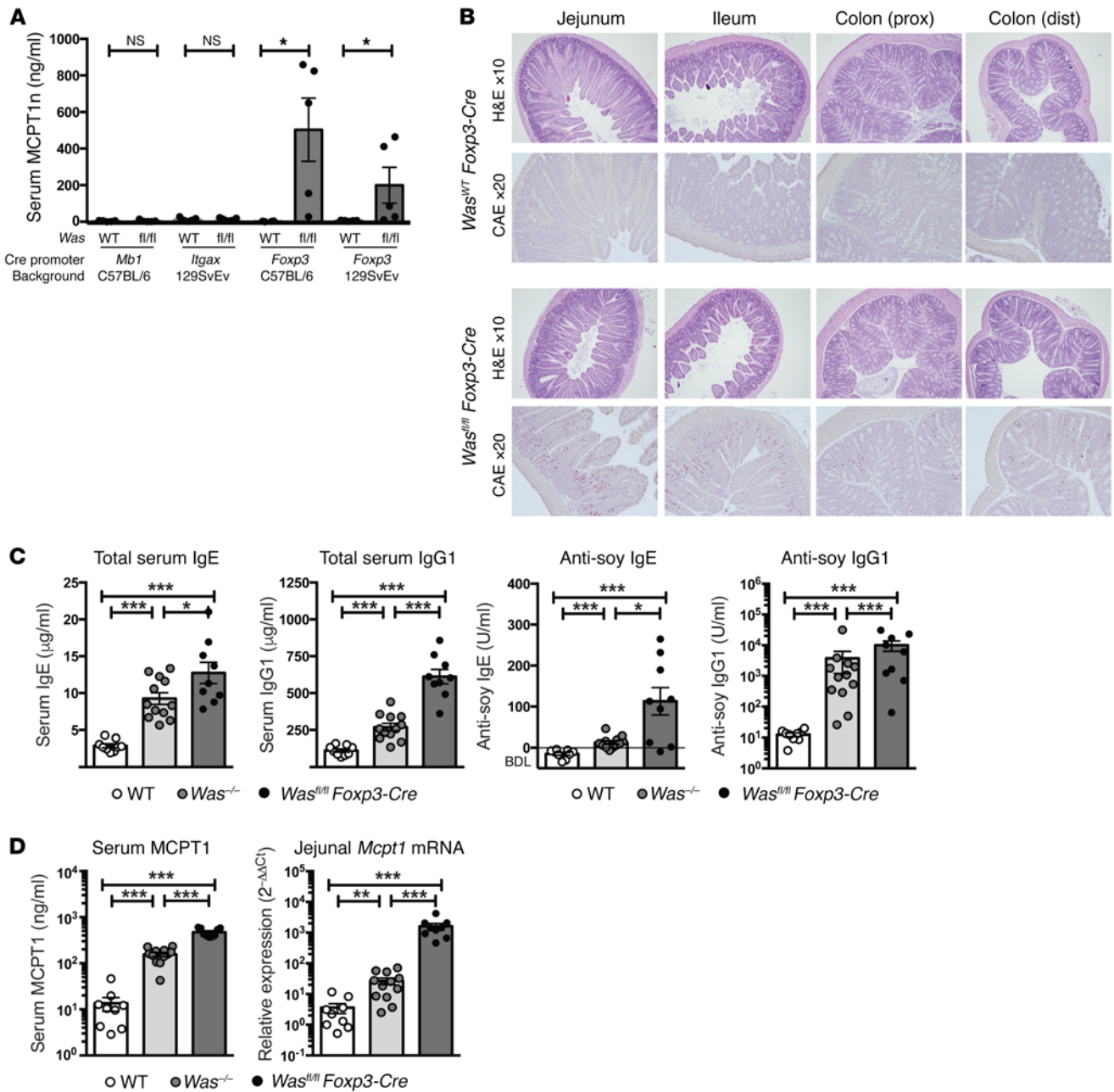
Figure 4. WASP deficiency in Tregs is sufficient for the development of spontaneous food allergy and results in more severe disease. (**A**) Comparison of MCPT1 levels in mice with cell type–specific WASP deletions. Mice with conditional deletion of $Was^{fl/fl}$ alleles in B cells ($Was^{fl/fl}$ $Mb1$-Cre), CD11c⁺ dendritic cells ($Was^{fl/fl}$ $Itgax$-Cre) or Tregs ($Was^{fl/fl}$ $Foxp3$-Cre) of ≥ 2 months of age, $n ≥ 5$ per group. (**B**) Representative H&E (×10 magnification) and chloroacetate esterase (CAE) staining (×20 magnification) of intestinal cross-sections in $Was^{fl/fl}$ $Foxp3$-Cre or Was^{WT} $Foxp3$-Cre littermates on the C57BL/6 background. (**C**) Comparison of total and soy-specific IgE and IgG1 at 2 months in cohoused WT (open circles, $n = 9$), $Was^{−/−}$ (gray circles, $n = 12$), and $Was^{fl/fl}$ $Foxp3$-Cre (black circles, $n = 9$) mice of mixed genders on the C57BL/6 background. (**D**) Comparison of serum protein and jejunal mRNA expression levels of mucosal mast cell marker MCPT1. Symbols represent individual mice and error bars depict SEM. *$P < 0.05$, **$P < 0.01$, ***$P < 0.001$. NS, not significant as determined by 2-tailed Student's t test (**A**) or 1-way ANOVA with Tukey's multiple comparisons test (**C** and **D**). BDL, below detection limit. Data in **C** and **D** are representative of 2 independent cohorts.

whether WASP deficiency in other immune compartments contributed further to the pathogenesis of food allergic sensitization. Comparison of cohoused, age-, and sex-matched $Was^{fl/fl}$ $Foxp3$-Cre, $Was^{−/−}$, and WT animals revealed that $Was^{fl/fl}$ $Foxp3$-Cre mice developed higher levels of total and soy-specific IgE and IgG1 (Figure 4C) as well as higher serum MCPT1 levels and increased

intestinal $Mcpt1$ mRNA expression (Figure 4D) than mice with complete deletion of WASP. More severe allergic intestinal inflammation was confirmed by digital mRNA expression profiling on jejunal tissue, which revealed a type 2 immune cluster that contained multiple mast cell markers in addition to $Mcpt1$, including $Mcpt2$, $Fcer1a$, $Fcer1b$, and $Cpa3$ together with Th2-type cytokines
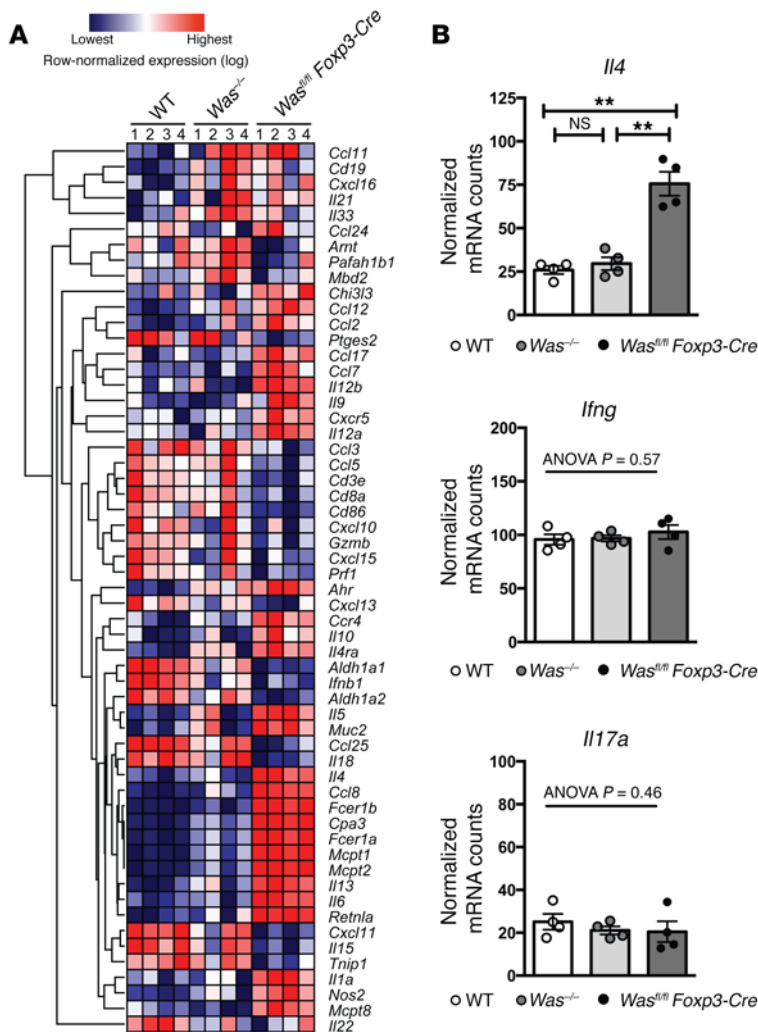
Figure 5. WASP deficiency in Tregs results in Th2-type small intestinal inflammation. (**A**) Hierarchical cluster analysis of differentially expressed genes within a panel of 86 inflammatory targets in tissue sections obtained from jejunum of cohoused female mice. Row-normalized, log-transformed mRNA counts are shown from 4 animals per group. (**B**) Bar graph representation and statistical analysis of mRNA expression of *Il4*, *Ifng*, and *Il17a* in jejunal sections as shown in **A**. Symbols represent individual mice and error bars depict SEM. **$P < 0.01$. NS, not significant as determined by 1-way ANOVA with Tukey's multiple comparisons test.

to or higher than those of WT counterparts (Figure 6A and Supplemental Figure 4A). This increase in Treg numbers compared with those in *Was*^{-/-} mice could have been due to higher levels of IL-2, since CD4^{+} T cells from the MLNs of *Was*^{fl/fl} *Foxp3-Cre* mice were found to produce WT levels of IL-2 upon anti-CD3/CD28 stimulation (Figure 6B). We reasoned that a relative underrepresentation of iTregs, which particularly control tolerance to foreign antigens (9), could potentially underlie the occurrence of IgE-mediated immune responses to food antigens. However, cell-surface staining of neuropilin-1, the absence of which specifically defines iTregs (43, 44), revealed that iTregs made up equivalent fractions of total FOXP3^{+} Tregs in WT, *Was*^{-/-}, and *Was*^{fl/fl} *Foxp3-Cre* mice (Supplemental Figure 4B). Similarly, we found no differences in the activation status of Tregs, as *Was*^{fl/fl} *Foxp3-Cre* and WT mice showed equal fractions of CD44^{hi}CD62L^{lo} effector memory Tregs (Supplemental Figure 4C).

Despite these normal numerical and phenotypical characteristics of WASP-deficient FOXP3^{+} Tregs, we observed that both *Was*^{-/-} and *Was*^{fl/fl} *Foxp3-Cre* mice developed a mild CD4^{+} lymphoproliferation in MLNs (Figure 6C). Within this expanded CD4^{+} T cell pool in MLNs of *Was*^{-/-} and *Was*^{fl/fl} *Foxp3-Cre* mice, an increased fraction of cells displayed the CD44^{hi}CD62L^{lo} effector memory T cell phenotype. Within this latter fraction, we observed an increase in Th2-skewed effector T cells, as determined by their coexpression of ICOS and the Th2 transcription factor GATA3 (45, 46) (Figure 6D and Supplemental Figure 4D). In sharp contrast, the fraction of Th1-skewed, T-bet[+] effector T cells was decreased in *Was*^{fl/fl} *Foxp3-Cre* mice, whereas the abundance of Th17-skewed, RORγt^{+} T cells was equivalent among all 3 genotypes (Figure 6E). This selective Th2 skew in the CD4 effector compartment was corroborated further by analysis of cytokine production from CD4^{+} mesenteric lymphocytes cultured ex vivo, which showed significantly increased production of IL-4 and IL-13, whereas IFN-γ and IL-17 production was similar to that of WT mice in both *Was*^{-/-} and *Was*^{fl/fl} *Foxp3-Cre* animals (Figure 6F). These results demonstrated that WASP-deficient Tregs are capable of normally regulating Th1 or Th17 differentiation, but fail to specifically contain Th2 effector responses in vivo.

We then aimed to investigate whether WASP-deficient FOXP3^{+} Tregs were selective in their capacity to suppress Th1-, Th2-, or Th17-polarized effector cells in vitro. To do this, we first isolated congenically marked CD45.1^{+} naive CD4^{+} T cells and polarized
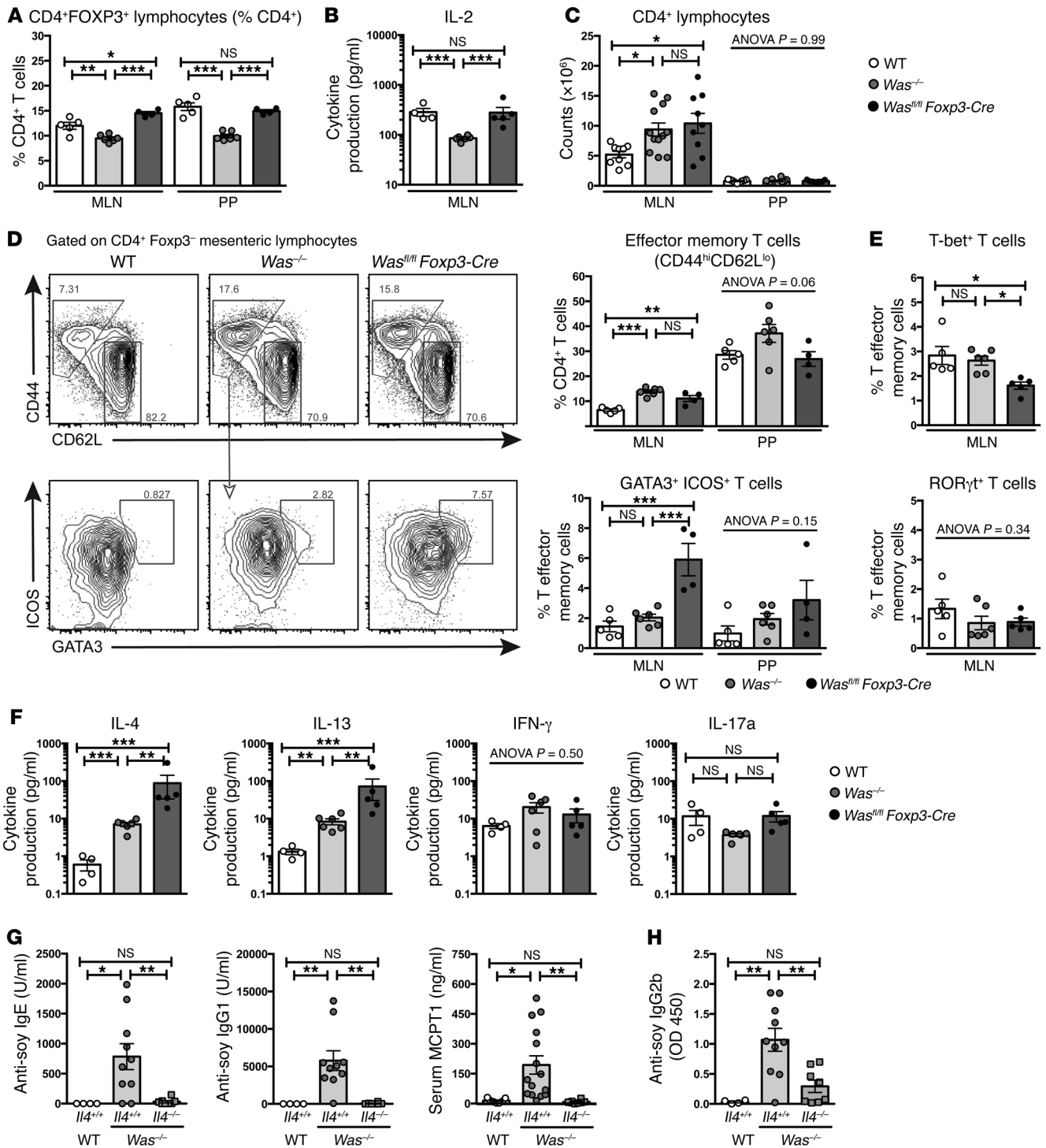
Il4, *Il13*, and *Il5* that were more prominently expressed in *Was*^{fl/fl} *Foxp3-Cre* than *Was*^{-/-} mice (Figure 5A and Supplemental Figure 3B). This analysis indicated that jejunal inflammation was Th2 specific, since mRNA levels of *Ifng*, *Il17a*, and *Tnfa* in the small intestine were equivalent to WT levels in both *Was*^{-/-} and *Was*^{fl/fl} *Foxp3-Cre* mice (Figure 5B and Supplemental Figure 3B). Taken together, these results demonstrate that conditional deletion of WASP in FOXP3^{+} Tregs resulted in increased development of IgE-mediated immune responses to food antigens and Th2-specific small intestinal tissue inflammation.

WASP-deficient Tregs fail to selectively suppress Th2 effector responses in vivo. *Was*^{-/-} animals are known to have reduced FOXP3^{+} Treg numbers, and WASP-deficient Tregs exhibit aberrant proliferation and suppression in response to TCR stimulation in vitro (39, 41, 42). These abnormalities, which can be partly attributed to reduced levels of IL-2, have previously been associated with the occurrence of autoimmunity and colitis in *Was*^{-/-} mice (39, 41). The sequelae of Treg-conditional WASP deficiency on intestinal immune homeostasis, however, have thus far remained undefined.

In sharp contrast to *Was*^{-/-} mice, both relative and absolute FOXP3^{+} Treg numbers in the mesenteric lymph nodes (MLNs) and Peyer's patches (PPs) of *Was*^{fl/fl} *Foxp3-Cre* mice were equal

Figure 6. WASP-deficient FOXP3+ Tregs fail to suppress Th2-type lymphoproliferation in vivo. (**A**) Quantification by flow cytometry of FOXP3+ Tregs amongst CD4+ T cells obtained from MLNs or PPs of WT (open circles, *n* = 5), *Was−/−* (gray circles, *n* = 6) and *Was^fl/fl^ Foxp3-Cre* (black circles, *n* = 4) mice. (**B**) Production of IL-2 by CD4+ mesenteric T lymphocytes stimulated with anti-CD3/CD28 ex vivo. Each dot represents the average cytokine production from triplicate cell suspensions from a single mouse. (**C**) Total CD4+ T cell numbers obtained from MLNs and PPs. (**D**) Gating strategy of GATA3+ICOS+ Th2-type effector cells within the parent gate of effector memory T cells from MLNs of representative samples, with quantification and statistical testing in the right panels. (**E**) Fraction of T-bet+ and RORγt+ effector memory T cells. (**F**) Production of IL-4, IL-13, IFN-γ and IL-17a by CD4+ mesenteric T lymphocytes stimulated with anti-CD3/CD28 ex vivo. Each data point represents the average cytokine production from triplicate cell suspensions from a single mouse. (**G**) Serum levels of anti-soy specific IgE and IgG1, and MCPT1 in *Was−/−* mice on the 129SvEv background with either *Il4+/+* (gray circles, *n* = 10 or 15) or *Il4−/−* alleles (gray squares, *n* = 8). (**H**) Anti-soy IgG2b titer as determined by ELISA in 1:1,000 serum dilution. Symbols represent individual mice and error bars depict SEM. *$P < 0.05$, **$P < 0.01$, ***$P < 0.001$. NS, not significant as determined by 2-tailed Student's *t* test or 1-way ANOVA with Tukey's multiple comparisons test. In **B** and **F**, data were log-transformed prior to statistical testing. Data from 2 pooled experiments (**C**, **G**, and **H**) or representative results from ≥ 2 independent experiments (**A**, **B**, and **D**–**F**) are shown.

them into Th1, Th2, or Th17 effector subsets (Supplemental Figure 5A). We confirmed the identity of the polarized cells by staining for Th-specific transcription factors T-bet, GATA3, and RORγt (Supplemental Figure 5B). We then CFSE labeled these responder cells and cocultured them with sorted EGFP$^+$ Tregs from *Was$^{+/+}$ Foxp3-Cre* or *Was$^{fl/fl}$ Foxp3-Cre* mice (Supplemental Figure 5C) in the presence of αCD3/αCD28 and examined CD45.1$^+$ responder cell proliferation 72 hours later (Supplemental Figure 5D). Both WT and WASP-deficient FOXP3$^+$ cells proved equally poor in their ability to suppress in vitro–polarized effector cells (Supplemental Figure 5D) even though the WT Tregs were competent in suppressing naive T cell proliferation (Supplemental Figure 5E). With this set of experiments, we were therefore unable to demonstrate that the selective loss of Th2 suppression by WASP-deficient Tregs in vivo also occurs with cocultured polarized cells in vitro.

We next assessed the pertinence of the Th2 cytokine IL-4 on the pathogenesis of food allergy in *Was$^{-/-}$* mice, by analyzing the extent to which food-allergic sensitization occurred in *Was$^{-/-}$ Il4$^{-/-}$* animals. Antisoy, as well as total IgE and IgG1, responses were completely abrogated in the absence of IL-4, and mucosal mast cell expansion and activation did not occur as assessed by serum MCPT1 levels (Figure 6G and Supplemental Figure 4E). Furthermore, antisoy titers of the IL-4–independent IgG2b isotype were also significantly lower in *Was$^{-/-}$ Il4$^{-/-}$* mice (Figure 6H), signifying a critical role for Th2-mediated inflammation in the induction of antifood humoral immune responses in WASP-deficient mice.

WASP-deficient effector Tregs assume a Th2-like phenotype. Recent data indicate a role for Th2-type–programmed Tregs in an experimental model of murine food allergy as well as human children (47). Similarly, a Th2-promoting fraction of Tregs that depends on TCR signaling was identified in asthmatic mice and patients (48). Since aberrant responses to TCR activation are a feature of WASP-deficient T cells (49), we analyzed the extent to which WASP-deficient Tregs display a Th2-like phenotype. In both *Was$^{-/-}$* and *Was$^{fl/fl}$ Foxp3-Cre* mice, we observed increased fractions of GATA3$^+$ICOS$^+$ Tregs in MLNs compared with WT counterparts (Figure 7A and Supplemental Figure 6A). These cells were confined to the CD44^{hi}CD62L^{lo} effector-like Treg subset, as GATA3 expression in the naive-like fraction of Tregs was equivalent to WT CD4$^+$FOXP3$^+$CD44^{lo}CD62L^{hi} Tregs (Figure 7B). Th2-type reprogrammed Tregs in the context of food allergy had previously been observed in a genetic model that relies on increased signaling through the IL-4 receptor (47). We therefore asked whether WASP-deficient CD44^{lo}CD62L^{hi} Tregs exhibit an increase in GATA3 expression pattern in response to increased availability of IL-4 in a Th2-skewed inflammatory setting. However, analysis of *Was$^{-/-}$ Il4$^{-/-}$* animals revealed that, while Th2 skewing of effector T cells and IL-4 production from CD4$^+$ mesenteric lymphocytes was abrogated (Figure 7C), an equivalent increase in the fractions of GATA3$^+$ICOS$^+$ memory-effector Tregs was found when compared with *Was$^{-/-}$* IL-4–competent counterparts, while relative Treg numbers were similar between groups (Figure 7D and Supplemental Figure 6B). Additional analysis revealed that increased expression of transcription factors did not extend to T-bet or RORγt, as memory-effector Tregs coexpressing these markers were found in similar frequencies among all genotypes (Figure 7D). When naive T cells were stimulated with anti-CD3/CD28 and TGF-β

in vitro, we observed no difference in the induction of GATA3$^+$ Tregs from WT or *Was$^{fl/fl}$ Foxp3-Cre* donor-derived cells (Supplemental Figure 6C), indicating that differentiation into the Treg lineage in the absence of WASP by itself is insufficient to cause increased GATA3$^+$ expression. This suggests that the appearance of GATA3$^+$ICOS$^+$ Tregs depends on additional external signals in vivo. Combined, these data demonstrate that WASP-deficient effector memory Tregs, but not naive-like Tregs, assume a Th2-like phenotype independently from increased IL-4 signaling.

Finally, we determined whether GATA3$^+$ Tregs are increased in patients with mutations in *WAS*. Individuals with either XLT or WAS displayed increased fractions of GATA3$^+$ Tregs among the effector Tregs isolated from peripheral blood mononuclear cells (PBMCs) (Figure 7E). Similarly, the mean fluorescence intensity of GATA3 was higher in effector Tregs from WAS and XLT patients than in age-matched, male controls (Supplemental Figure 6D). Interestingly, we observed a correlation between severity of *WAS* mutation and GATA3 expression in Tregs, as the fraction of GATA3$^+$ Tregs was significantly ($P < 0.05$; multiplicity adjusted P value = 0.015) higher in WAS patients than in individuals with XLT. In agreement with our observations in mice, WAS patients also had a higher fraction of FOXP3$^-$GATA3$^+$ effector T cells (Th2 cells, Supplemental Figure 6E). Three WAS patients who had previously undergone HSCT showed a normal GATA3$^+$ effector Treg compartment as well as Th2 effector cells among PBMCs (Figure 7E and Supplemental Figure 6E). These results indicate that loss of suppression of Th2 effector responses and assumption of a Th2-type phenotype of Tregs also occur in human WAS patients.

Discussion

WAS is an illustrative example of how investigating a monogenetic human disease can advance our understanding of immune pathways in health and disease (16, 19). Data from *Was$^{-/-}$* mice (26) revealed that WASP-dependent functions are highly conserved between mouse and human and that many aspects of the human disease are faithfully mimicked in these animals. WASP is best characterized for its role as stimulator of ARP2/3-mediated actin polymerization, which enables a variety of downstream effector functions including tissue migration and filopodia stability. A vast body of literature has accumulated that addresses the molecular and immunological consequences of deficiency of WASP in not just T and B lymphocytes, but also invariant NKT (iNKT) cells, platelets, NK cells, mast cells, dendritic cells, monocytes, and neutrophils (50). Because many of these WASP-dependent functions have been defined in either patients and mice lacking WASP in all hematopoietic lineages or in isolated cell systems ex vivo or in vitro, the systemic sequelae of cell-specific perturbations in WASP-mediated signals has remained largely unknown (50).

Here, we report an increased prevalence of allergic responses against common food antigens as a feature of WAS in humans. Although elevated levels of sIgE and eczema are well-described characteristics of the disease, the burden of IgE-mediated allergic disorders among patients with WAS or XLT has remained largely uncharacterized. Our studies demonstrate that the elevated sIgE pool in these patients is functional and has the capacity to mediate allergic reactions to common food antigens, which should prompt treating physicians to be vigilant for food allergy among
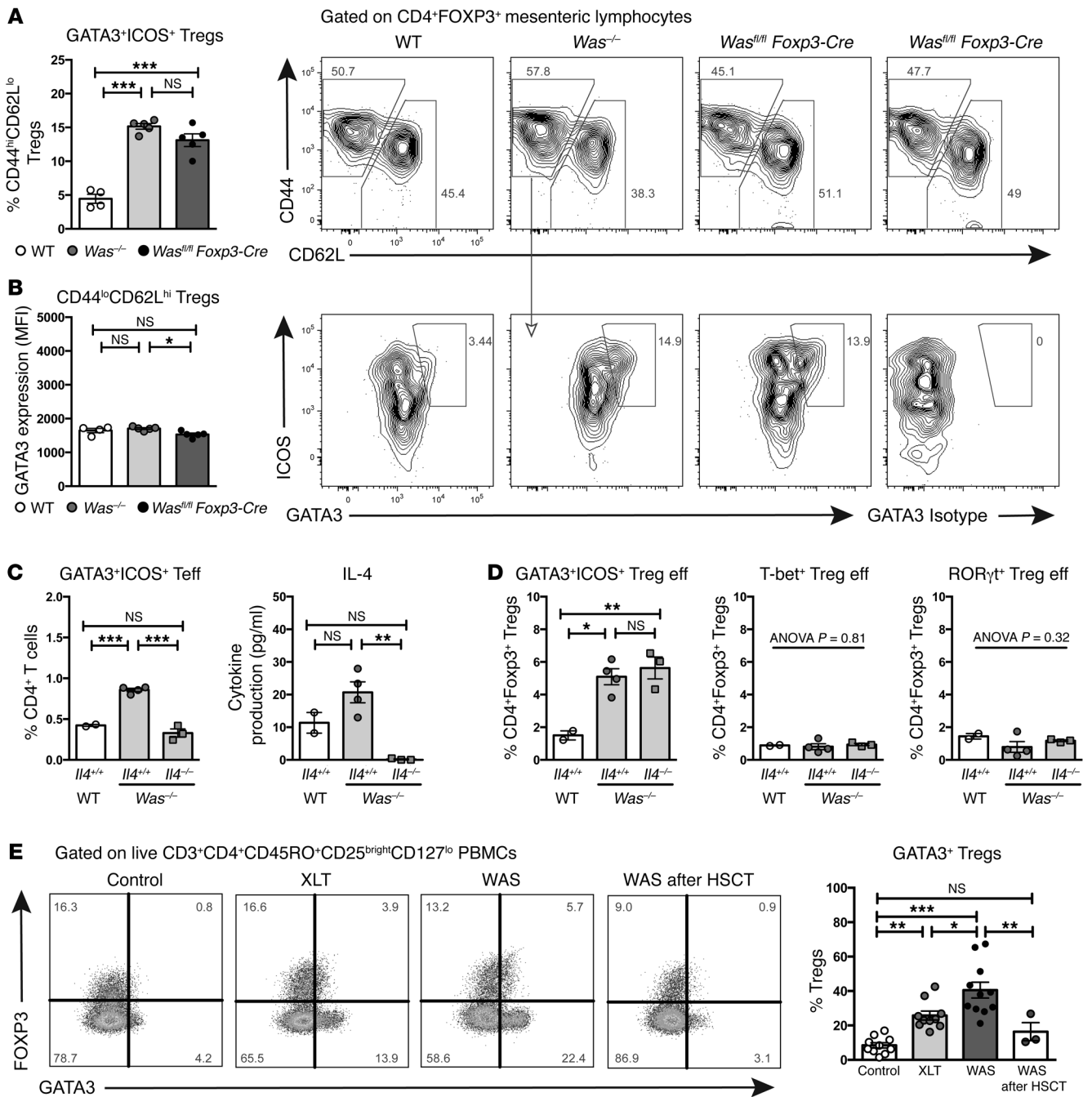
Figure 7. WASP-deficient effector Tregs assume a Th2-like phenotype in mice and human patients. (**A**) Fraction of CD44hiCD62LloCD4+FOXP3+ Tregs that coexpress GATA3 and ICOS in WT (open circles, *n* = 4), *Was⁻/⁻* (gray circles, *n* = 6) and *Wasfl/fl Foxp3-Cre* (black circles, *n* = 5) mice, with gating strategy in representative samples depicted on the right. (**B**) Intracellular GATA3 levels in CD44loCD62LhiCD4+FOXP3+ Tregs determined by mean fluorescence intensity (MFI) using flow cytometry. (**C**) GATA3+ICOS+ effector T cells in WT or *Was⁻/⁻* mice with either *Il4+/+* (gray circles, *n* = 4) or *Il4⁻/⁻* alleles (gray squares, *n* = 3) and IL-4 production by CD4+ mesenteric lymphocytes stimulated with anti-CD3/CD28 ex vivo. Each data point represents the average cytokine production from triplicate cell suspensions from a single mouse. (**D**) Percentage of FOXP3+ Tregs coexpressing GATA3 and ICOS, T-bet, or RORgt in WT or *Was⁻/⁻* mice with either *Il4+/+* or *Il4⁻/⁻* alleles. (**E**) Gating strategy and cumulative data of percentage of total effector (CD45RO+) Tregs coexpressing GATA3 in isolated PBMCs from XLT (*n* = 10) and WAS (*n* = 11) patients compared with age- and sex-matched controls (*n* = 10) or WAS patients following HSCT (*n* = 3). Data points represent individual mice or patients and error bars depict SEM. *P < 0.05, **P < 0.01, ***P < 0.001. NS, not significant as determined by 1-way ANOVA with Tukey's multiple comparisons test. Mouse experiments representative of 2 independent experiments. Results in **E** are cumulative data from 1 experiment.

these patients and to obtain a careful history of adverse events after food ingestion.

The connection between WASP deficiency and the occurrence of IgE-mediated reactions against foods was further corroborated by studies in *Was⁻/⁻* animals. WASP-deficient mice produce IgE and IgG1 antibodies with specificity for components of chow, most prominently soy and wheat, which are also 2 allergens commonly implicated in IgE-mediated food allergy in human patients

(51, 52). These responses were observed in *Was*^{−/−} mice on 3 different genetic backgrounds, independent of colonic inflammation, and occurred similarly in mice that were housed under GF settings when compared with those colonized with an SPF flora. As such, our findings suggest that mutations in *Was* predispose to allergic disease independently of microbe-derived signals or differences in strain-specific immune constitution.

Using a loxP/Cre-based system permitting cell-specific deletion of WASP (53), we demonstrated that FOXP3^{+} Tregs are critically dependent on WASP-mediated signals for their ability to maintain tolerance to ingested food antigens. These results indicate that WASP deficiency in other immune compartments such as antigen-presenting cells, B cells, or effector CD4^{+} T cells is dispensable for the pathogenesis of food-allergic responses in *Was*^{−/−} mice and, potentially, WAS patients. In fact, the absence of WASP in non-FOXP3^{+} immune cells is likely to have a net dampening effect on IgE sensitization to food antigens, since both food-specific IgE titers and allergic intestinal tissue inflammation were markedly lower in *Was*^{−/−} mice when compared with *Was*^{fl/fl} *Foxp3-Cre* mice. In support of this conclusion, work by Morales-Tirado et al. previously identified a Th2-specific dysfunction of WASP-deficient CD4^{+} effector T cells, manifesting as a reduced production of IL-4 and compromised expulsion of *Nippostrongylus brasiliensis* (54). Indeed, following ex vivo TCR stimulation, we confirmed reduced production of IL-4 and IL-13 by CD4^{+} mesenteric lymphocytes obtained from *Was*^{−/−} mice when compared with cells from *Was*^{fl/fl} *Foxp3-Cre* mice. In human WAS patients, which are more likely to resemble *Was*^{−/−} mice than *Was*^{fl/fl} *Foxp3-Cre* animals, reduced effector function in Th2 lymphocytes may account for the observation that only 20%–30% of WAS and XLT patients in our cohort suffer from clinically relevant food allergy. Notably, none of the food-allergic patients suffered from anaphylaxis upon allergen exposure, which may be related to reduced mast cell histamine secretion in response to IgE-mediated activation, as has been previously described for WASP-deficient mice (55). Using morphine as an antigen/IgE-independent mast cell stimulus, we observed reduced wheal responses in WAS patients when compared with controls. Together with the high discordance between sIgE levels and SPT in patients with mutations in *WAS*, with several false-negative SPT results, these data suggest that mast cell dysfunction may contribute further to the moderate allergic phenotype in WAS patients and in *Was*^{−/−} mice when compared with *Was*^{fl/fl} *Foxp3-Cre* animals.

Previous studies on Tregs in *Was*^{−/−} mice have hypothesized that the immunopathology in these animals results in part from reduced numbers of FOXP3^{+}CD4^{+} lymphocytes in secondary lymphoid organs (39, 41, 42). However, we found that conditional deletion of WASP in *Was*^{fl/fl} *Foxp3-Cre* mice did not lead to lower Treg numbers in PPs or MLNs when compared with WT animals. These findings implicate functional abnormalities in WASP-deficient Tregs as the principal cause of immune dysregulation in *Was*^{−/−} mice. Although these Treg abnormalities manifest in vivo as an inability to control Th2 effector cells, in vitro suppression assays showed that WASP-deficient Tregs were unable to suppress other effector cell subsets as well. The basis for this difference is not yet understood. In further support of a Treg-intrinsic role for WASP in controlling aberrant immune responses, we observed increased expression of the Th2 transcription factor GATA3 in activated WASP-deficient Tregs from either *Was*^{fl/fl} *Foxp3-Cre* or *Was*^{−/−} hosts when compared with WT animals and similarly in human patients with WAS in comparison with age- and sex-matched controls.

Although the molecular mechanism of Treg-specific dysfunction in the absence of WASP remains to be elucidated, emerging data suggest aberrant signaling downstream of TCR ligation as a possible candidate. Increased Th2 responses and elevated IgE also result from loss of function of the TCR-associated scaffold protein LAT (56, 57). WASP is rapidly recruited to the TCR upon ligation (58) and is required for internalization of the TCR complex (59). Since Tregs have been shown to require continuous TCR-dependent signaling for optimal suppressive function (60, 61), alterations in downstream events following TCR-mediated activation in the absence of WASP may be related to the loss of Th2-suppressive capacity. Moreover, deficiency of the TCR-associated phosphatase SHP-1 results in an increased population of GATA3^{+} Tregs and food allergy similar to our observations in patients and mice with WASP deficiency (47). Together, these findings support a link between aberrant TCR signaling in WASP-deficient Tregs and unrestrained Th2 pathology in vivo. However, our studies also indicate that disruption of TCR-mediated signals in WASP-deficient effector T cells is not required for Th2-skewed immune responses to occur, as *Was*^{fl/fl} *Foxp3-Cre* mice, which are sufficient for WASP in effector cells, showed increased numbers of GATA3^{+} effector T cells compared with *Was*^{−/−} animals. Molecular profiling and immune phenotyping of WASP-deficient Tregs following TCR-mediated activation may further elucidate the mechanism that results in a Th2-skewed regulatory phenotype.

In summary, we identified an increased prevalence of IgE-mediated food allergy among a cohort of patients with mutations in *WAS*. Using *Was*^{−/−} mice, we showed that IgE sensitization occurs both in the presence and absence of an intestinal flora and that the deficiency of WASP in FOXP3^{+} Tregs alone is sufficient to drive allergic intestinal inflammation. While capable of fully containing Th1 and Th17 effector responses in vivo, WASP-deficient Tregs exhibit a Th2-like phenotype and fail to selectively restrain Th2 effector differentiation, resulting in intestinal mast cell expansion and activation. Our findings demonstrate that in WAS, defective FOXP3^{+} Tregs promote Th2-type immune hyperactivation and allergic disease.

Methods

Patients. Twenty-five consecutive patients with WAS or XLT followed by NHGRI on an active clinical protocol (NCT00006319), provided informed consent on an NIH IRB-approved research protocol designed to study atopy (NCT01164241). Prior to enrollment, a clinical diagnosis of WAS or XLT was confirmed by mutation analysis of the *WAS* gene and WASP expression as previously described (62). Comprehensive allergic histories, review of all available outside records pertaining to prior allergic or immunologic evaluation and therapeutic intervention, as well as physical examinations were performed at the Clinical Center of the NIH. Total and allergen-specific sIgE levels were quantified by ImmunoCAP (Phadia) from all patients (*n* = 25). SPT of a panel of common allergens was performed in patients with sufficient intact/noninflamed skin (*n* = 14) and compared with standard clinical positive and negative controls. Because 3 individuals had

previously undergone HSCT, data from sera and SPTs were excluded from analysis. SPT to morphine (10, 3, 1, 0.3, and 0.1 mg/ml) was performed in individuals with WAS mutations (n = 13) and compared with control subjects (n = 15).

Animals. The generation of *Was*^{−/−}, *Was*^{−/−} *Il4*^{−/−}, and *Was*^{−/−} *Rag2*^{−/−} mice has been previously described (26, 27) and *Was*^{−/−} animals have since been made commercially available from The Jackson Laboratory. All mice used in this study were bred in house and maintained in accordance with institutional guidelines in SPF conditions at the Boston Children's Hospital. 129SvEv *Was*^{−/−} animals were rederived into GF conditions at Boston Children's Hospital. The C57BL/6 mice harboring floxed *Was* alleles (*Was*^{fl/fl} females or *Was*[fl/] males) were generated and donated by Adrian Thrasher (University College London Institute of Child Health) as previously described (53). We backcrossed these mice for 10 generations onto the 129SvEv background in our facility. *Itgax-Cre* mice and *Foxp3-Cre* mice on the C57BL/6 background were obtained from The Jackson laboratory and backcrossed for at least 10 generations onto the 129SvEv background. Serum from *Was*[fl/] *Mb1-Cre* and *Was*[WT] *Mb1-Cre* animals was provided by Stefano Volpi and Luigi Notarangelo at the Department of Immunology of Boston Children's Hospital.

Chow and chow extracts. All mice were kept on irradiated Prolab Isopro RMH 3000 (LabDiet) throughout their lives. Crude samples of the 5 main (% w/w) components (in order of abundance: ground wheat, soybean meal, wheat middlings, ground yellow corn, and fish meal) were obtained directly from LabDiet. Protein extracts for in vitro studies were generated by soaking approximately 10 grams of homogenized chow pellets or meal component in 40 ml of phosphate-buffered saline (PBS) in a 50-ml Falcon tube, which was placed in a shaking incubator at 37°C for 4 hours, and then spun at 5,000 *g* for 10 minutes. The supernatant containing solubilized food antigens was then ultracentrifuged (100,000 *g*) for 1 hour and sterile-filtered using a 20-micron syringe filter (Corning). Protein concentration of extracts was quantified using a colorimetric protein assay (Bio-Rad). For allergen elimination experiments, mice were transferred to a clean cage containing a protein-free, amino acid–based formula (Research Diets Inc.). An elemental chow extract was obtained from mortar-and-pestle-homogenized pellets as described for regular chow.

ELISAs. Total and ovalbumin-specific (OVA-specific) IgE and IgG1 ELISAs were performed as previously described (34) using the following reagents. Capture antibodies: anti–mouse IgE (Southern Biotech, catalog 1110-01) and anti–mouse IgG1 (Southern Biotech, catalog 1070-01). Protein standards: mouse IgE and IgG1 κ isotype controls (BD Pharmingen) and mouse anti-OVA IgE (AbD Serotec, catalog MCA2259). Detection reagents: horseradish peroxidase–conjugated anti–mouse IgE (Southern Biotech, catalog 1110-05) and IgG1 (Southern Biotech, catalog 1070-05), biotin-conjugated OVA (US Biologicals), and streptavidin-conjugated horseradish peroxidase (BD Pharmingen).

For food-specific Ig ELISAs, 96-well polystyrene plates (Costar assay plates, Corning) were coated overnight with 100 μl of food extract in PBS (100 μg/ml protein concentration). Plates were subsequently washed 6 times with 300 μl of 0.05% Tween in PBS (washing buffer) and blocked with 10% fetal calf serum (FCS) in PBS for a minimum of 2 hours at room temperature. Serum dilutions ranging from 1:30 to 1:5,000 were prepared in 2% FCS in PBS and transferred to wells in a volume of 100 μl. Plates were incubated at room temperature for 3 hours and then washed again 6 times in washing buffer, after which anti-food Ig antibodies were detected with horseradish peroxi-

dase-conjugated antibodies against IgE (catalog 1110-05), IgG1 (catalog 1070-05), IgG2a (catalog 1080-05), IgG2b (catalog 1090-05), IgG3 (catalog 1100-05), or IgA (catalog 1040-05) (all from Southern Biotech) in 1:1,000 dilutions in 2% FCS in PBS for 1 hour at room temperature. Following 6 additional washes, plates were developed in the dark for 3–10 minutes with 100 μl of tetramethylenbenzidine per well (KPL). This reaction was stopped by the addition of 50 μl of 2 M H_2SO_4 prior to spectrophotometric analysis at 450 nm (PerkinElmer). To allow semi-quantitative comparison of reactivity against different food extracts, all 5 investigated extracts were coated in equivalent concentrations in adjacent wells on the same 96-well plate. For each sample, a sixth well was included that was coated with PBS alone and the OD of this blank well was subtracted from the OD of the extract-coated wells to correct for any nonspecific binding and thus obtain the Ig reactivity against any of the 5 components. Cumulative anti-food Ig titers were defined as the sum of the blanked OD values of all 5 investigated extracts. For some experiments, wells were coated with combined wheat and soy extracts, and 2-fold serial dilutions of a positive serum sample were used to quantify the anti-food IgG1 reactivity as arbitrary units/ml (U/ml).

Serum MCPT1, as well as IL-4, IL-13, IL-2, IL-17a, and IFN-γ ELISAs were performed using a commercially available kit (eBioscience) according to the manufacturer's instructions.

Flow cytometric analysis. To assess basophil-surface IgE loading, whole-blood samples were collected in EDTA. Following lysis of erythrocytes in RBC lysis buffer (eBioscience), cell pellets were blocked with anti–mouse CD16/CD32 (clone 2.4G2, BD Pharmingen) and stained with anti–mouse CD45 (clone 30-F11), anti–mouse CD49b (clone DX5), anti–mouse FcεRIa (clone MAR-1), and anti–mouse IgE (clone RME-1, all from Biolegend). Basophils were identified within PBMCs as CD45[Mid]CD49b^{+}FcεRIa^{+}IgE^{+}, and IgE surface loading was determined from the mean fluorescence intensity of the anti-IgE stain. Immune profiling of MLN and PP lymphocytes was performed using the following fluorochrome-conjugated antibodies: anti-CD4 (Biolegend, clone GK1.5), anti-FOXP3 (eBioscience, clone FJK-16s), anti-GATA3 (eBioscience, clone TWAJ), anti-CD44 (Biolegend, clone IM7), anti-CD62L (Biolegend, clone MEL-14), anti-ICOS (Biolegend, clone C398.4A), anti–T-bet (c Biolegend, lone 4B10), anti-RORγt (eBioscience, clone B2D), anti–neuropilin-1 (R&D Systems, product number FAB556A), anti-CD16/CD32 (BD Pharmingen, clone 2.4G2), and Fixable Viability Dye eFluor 450 (eBioscience). Transcription factors were stained using the FOXP3/Transcription Factor Staining kit (eBioscience).

PBMCs from patients were isolated and regulatory CD4^{+} T cells were stained as previously described (63) with Live/Dead Fixable Blue viability dye (Invitrogen), anti-CD3 Alexa Fluor (AF)700, anti-CD25 phycoerythrin (PE)-Cy7, anti-CD127 AF647, anti-CD4 brilliant violet 605, anti-GATA3 AF488 (all from BD Biosciences), anti-CD45RO Texas Red-PE (Beckman Coulter), and anti-FOXP3 eFluor 450 (eBioscience).

Mast cell degranulation assays. Bone marrow–derived cells from WT BALB/c mice were differentiated to mast cells in vitro by culturing cells in RPMI 1640 medium (Gibco) supplemented with 10% FCS, 100 U/ml penicillin, 100 μg/ml streptomycin, 2 mM ʟ-glutamine, 50 μM β-mercaptoethanol, 10 ng/ml IL-3, and 20 ng/ml stem cell factor (SCF) (henceforth referred to as mast cell medium). Experiments were performed using cultures that were at least 8 weeks old and had a purity of greater than 90%, as assessed by cell surface coexpression of mast cell markers c-kit (clone 2B8) and FceRIa (clone MAR-1, both from Biolegend) by flow cytometry. Prior to degranulation assay, mast

cells were resuspended at 10^6/ml in mast cell medium and loaded overnight with dilutions of mouse serum in concentrations as indicated per experiment. The next day, cells were washed twice in medium, plated in a 96-well tissue culture plates (10^5 cells in 100 µl per well), and stained with viability dye. Cells were then challenged for 10 minutes with an antigen cocktail containing solubilized chow antigens (protein concentration 5 µg/ml) or OVA (500 ng/ml), in combination with anti–mouse LAMP-1 antibody (Biolegend, clone 1D4B). Following 2 washes with cold flow cytometry buffer (0.01% NaN_3 in PBS), cells were acquired on a FACSCanto II flow cytometer (BD Bioscience) and further analyzed using FlowJo software (Treestar).

Histology and mast cell staining. Following euthanasia, intestinal sections were isolated and flushed with cold PBS. Three jejunal sections per animal were fixed in formalin for 24 hours and then transferred to 70% ethanol. Tissue samples were paraffin embedded and sectioned by the Histology Core facility of Beth Israel Deaconess Medical Center, and mast cell quantification was performed as described (33). In brief, slides were deparaffinized in sequential xylene baths and rehydrated in graded alcohol solutions. Chloroacetate esterase staining solution consisted of 0.04% naphthol AS-D chloroacetate, 0.04% pararosaniline, and 0.04% sodium nitrite (all from Sigma-Aldrich) in PBS, and was used to stain slides for 30 minutes at room temperature. Slides were counterstained with modified Harris hematoxylin solution (Sigma-Aldrich) and mounted in Permount (Fisher). For statistical analysis, a blinded investigator counted mast cells in 4 randomly selected high-power fields. Images were captured using an Olympus DP70 microscope equipped with DP Controller software (Olympus).

Quantitative RT-PCR. Three jejunal tissue sections were pooled and stored in RNAlater (QIAGEN). Following tissue disruption and homogenization, total RNA was extracted using an RNeasy Plus minikit (QIAGEN) and reverse transcribed using iScript Supermix (Bio-Rad). *Mcpt1* gene expression was assessed with iQ SYBR Green Supermix (Bio-Rad) using the following primers: FOR 5′-GAGGACAGATGTG-GTGGGTTT-3′ and REV 5′-AGGAGTCAACTCAGCTTTCTCTT-3′, and normalized against expression of housekeeping gene *Hprt* (FOR 5′-GTTGGATACAGGCCAGACTTTGTTG-3′ and REV 5′-GAGG-GTAGGCTGGCCTATAGGCT-3′). Relative expression was determined using the $2^{-\Delta\Delta Ct}$ method, in which the ΔCt of a WT sample was set as reference value.

In vivo allergen challenge. To assess the occurrence of oral anaphylaxis, mice were starved for 3 hours and then challenged with 12.5 mg soy protein in 300 µl PBS by gavage. Body temperature was registered with the use of implantable temperature transponders (IPTT-300, Biomedic Data Systems). Baseline temperature was defined as the average of 3 measurements prior to challenge, and severity of anaphylaxis was assessed by calculating the ΔT from this average every 10 minutes after challenge.

Ex vivo culture and stimulation of mesenteric lymphocytes. Following isolation of MLNs, single-cell suspensions were purified using a MagniSort Mouse CD4+ T cell Enrichment Kit (eBioscience) according to the manufacturer's protocol and resuspended and plated in RPMI 1640 medium (Gibco) supplemented with 10% FCS, 100 U/ml penicillin, 100 µg/ml streptomycin, 2 mM L-glutamine, and 50 µM β-mercaptoethanol. Cytokine production was determined by ELISA in supernatants obtained in triplicates from 200,000 cultured cells per well that were stimulated for 18–24 hours with anti-CD3/CD28 using Dynabeads (Life Technologies).

In vitro polarization. Naive T cells were isolated from CD45.1 congenic C57BL/6 mice, stained using antibodies against anti-CD3 (clone 145-2C11), anti-CD4 (clone GK1.5), anti-CD25 (clone PC61), anti-CD44 (clone IM7) (all from BioLegend), and anti-CD62L clone MEL-14 and sorted based on CD3+CD4+CD25−CD44−CD62L+. Cells (2.5×10^5) were plated in a 24-well plate in RPMI 1640 medium (Gibco) supplemented with 10% FCS, 100 U/ml penicillin, 100 µg/ml streptomycin, 2 mM L-glutamine, 50 µM β-mercaptoethanol, and stimulated with plate-bound 5 µg/ml anti-CD3 (BD Pharmingen, clone 145-2C11) and 1 µg/ml anti-CD28 (BD Pharmingen, clone 16-0281-85) for 7 days in the presence of 20 ng/ml of IL-2 (Peprotech), 10 ng/ml IL-12 (R&D Systems), and 10 µg/ml anti–IL-4 (BD Pharmingen, clone 11B11) for Th1 polarization; 20 ng/ml of IL-2, 100 ng/ml IL-4, 10 µg/ml anti–IFN-γ (BD Pharmingen, clone XMG1.2), and 10 µg/ml anti–IL-12 (BD Pharmingen, clone C17.8) for Th2 polarization; 20 ng/ml of IL-6 (BioLegend), 2 ng/ml of human TGF-β (BioLegend), 10 µg/ml anti–IFN-γ, and 10 µg/ml anti–IL-4 for Th17 polarization.

Treg suppression assay. Following in vitro Th polarization, responder cells were labeled with CFSE and 5×10^4 cells were cocultured at a 1:1 ratio with sorted CD3+CD4+GFP+ Tregs isolated from *Was+/+ Foxp3-EGFP-Cre* or *Wasfl/fl Foxp3-EGFP-Cre* mice plated in a 96-well round-bottom plate in RPMI 1640 (Gibco) supplemented with 10% FCS, 100 U/ml penicillin, 100 µg/ml streptomycin, 2 mM L-glutamine, and 50 µM β-mercaptoethanol, and stimulated with αCD3/αCD28 Dynabeads (Life Technologies) for 3 days. Responder cell proliferation was analyzed by staining with anti-CD45.1 (BioLegend, clone A20) and assessing CFSE dilution using a 3-laser BD FACS-Canto II (BD Biosciences) flow cytometer.

In vitro Treg generation assay. CD3+CD4+CD25−GFP− naive T cells were sorted from *Was+/+ Foxp3-EGFP-Cre* and *Wasfl/fl Foxp3-EGFP-Cre* mice. Sorted cells (5×10^4) were plated in a 96-well plate in RPMI 1640 medium (Gibco) supplemented with 10% FCS, 100 U/ml penicillin, 100 µg/ml streptomycin, 2 mM L-glutamine, and 50 µM β-mercaptoethanol, and stimulated with anti-CD3/anti-CD28 Dynabeads (Life Technologies) in the presence of 2 ng/ml TFG-β (BioLegend) for 5 days. WT and *Was−/−* GFP+ iTregs were assessed for GATA3 expression using the 3-laser FACSCanto II.

Nanostring assay and hierarchical cluster analysis. Digital gene expression profiling was performed on isolated whole-tissue jejunal RNA as previously described using a customized Nanostring codeset consisting of 86 inflammatory targets and 5 housekeeping genes (34). Fifty-seven out of 86 investigated genes that were differentially expressed in any pairwise 2-sided *t* test comparison ($P < 0.05$) were subjected to hierarchical cluster analysis based on absolute Pearson correlation value with pairwise average linkage using the GenePattern algorithm (http://genepattern.broadinstitute.org).

Statistics. All results were analyzed and visualized using Prism version 6.0c for Mac (GraphPad Software). Details pertaining the use of specific statistical tests are provided in the figure legends. A *P* value of less than 0.05 was considered significant.

Study approval. All patients provided informed consent prior to inclusion in the study. Clinical studies were performed under an NIH IRB-approved research protocol (NCT01164241). All animal experiments were performed in accordance with Institutional Animal Care and Use Committee–approved protocol numbers 13-06-2415R and 14-04-2677R (IACUC, Boston Children's Hospital), and

Address correspondence to: Scott B. Snapper, 300 Longwood Avenue, EN670, Boston, Massachusetts 02115, USA. Phone: 617.919.4973; E-mail: scott.snapper@childrens.harvard.edu. Or to: Edda Fiebiger, 300 Longwood Avenue, EN626, Boston, Massachusetts 02115, USA. Phone: 617.919.2549; E-mail: edda.fiebiger@childrens.harvard.edu.

1. Wynn TA. Type 2 cytokines: mechanisms and therapeutic strategies. *Nat Rev Immunol*. 2015;15(5):271–282.
2. Pulendran B, Artis D. New paradigms in type 2 immunity. *Science*. 2012;337(6093):431–435.
3. Palm NW, Rosenstein RK, Medzhitov R. Allergic host defences. *Nature*. 2012;484(7395):465–472.
4. Ramsdell F, Ziegler SF. FOXP3 and scurfy: how it all began. *Nat Rev Immunol*. 2014;14(5):343–349.
5. Suscovich TJ, Perdue NR, Campbell DJ. Type-1 immunity drives early lethality in scurfy mice. *Eur J Immunol*. 2012;42(9):2305–2310.
6. Lin W, et al. Allergic dysregulation and hyperimmunoglobulinemia E in Foxp3 mutant mice. *J Allergy Clin Immunol*. 2005;116(5):1106–1115.
7. Akdis CA, Akdis M. Mechanisms and treatment of allergic disease in the big picture of regulatory T cells. *J Allergy Clin Immunol*. 2009;123(4):735–747.
8. Dhainaut M, et al. Thymus-derived regulatory T cells restrain pro-inflammatory Th1 responses by downregulating CD70 on dendritic cells. *EMBO J*. 2015;34(10):1336–1348.
9. Josefowicz SZ, et al. Extrathymically generated regulatory T cells control mucosal TH2 inflammation. *Nature*. 2012;482(7385):395–399.
10. Yu F, Sharma S, Edwards J, Feigenbaum L, Zhu J. Dynamic expression of transcription factors T-bet and GATA-3 by regulatory T cells maintains immunotolerance. *Nat Immunol*. 2015;16(2):197–206.
11. Li X, Zheng Y. Regulatory T cell identity: formation and maintenance. *Trends Immunol*. 2015;36(6):344–353.
12. Josefowicz SZ, Lu LF, Rudensky AY. Regulatory T cells: mechanisms of differentiation and function. *Annu Rev Immunol*. 2012;30:531–564.

13. Ozcan E, Notarangelo LD, Geha RS. Primary immune deficiencies with aberrant IgE production. *J Allergy Clin Immunol*. 2008; 122(6):1054–1063.
14. Altered T-cell receptor signaling in the pathogenesis of allergic disease. *J Allergy Clin Immunol*. 2011;127(2):351–354.
15. Yong PF, Freeman AF, Engelhardt KR, Holland S, Puck JM, Grimbacher B. An update on the hyper-IgE syndromes. *Arthritis Res Ther*. 2012;14(6):228.
16. Liston A, Enders A, Siggs OM. Unravelling the association of partial T-cell immunodeficiency and immune dysregulation. *Nat Rev Immunol*. 2008;8(7):545–558.
17. Sassi A, et al. Hypomorphic homozygous mutations in phosphoglucomutase 3 (PGM3) impair immunity and increase serum IgE levels. *J Allergy Clin Immunol*. 2014;133(5):1410–1419.e1.
18. Zhang Y, et al. Autosomal recessive phosphoglucomutase 3 (PGM3) mutations link glycosylation defects to atopy, immune deficiency, autoimmunity, and neurocognitive impairment. *J Allergy Clin Immunol*. 2014;133(5):1400–1409.e1.
19. Thrasher AJ, Burns SO. WASP: a key immunological multitasker. *Nat Rev Immunol*. 2010;10(3):182–192.
20. Snapper SB, Rosen FS. The Wiskott-Aldrich syndrome protein (WASP): roles in signaling and cytoskeletal organization. *Annu Rev Immunol*. 1999;17:905–929.
21. Albert MH, Notarangelo LD, Ochs HD. Clinical spectrum, pathophysiology and treatment of the Wiskott-Aldrich syndrome. *Curr Opin Hematol*. 2011;18(1):42–48.
22. Tuano KS, Orange JS, Sullivan K, Cunningham-Rundles C, Bonilla FA, Davis CM. Food

allergy in patients with primary immunodeficiency diseases: prevalence within the US Immunodeficiency Network (USIDNET). *J Allergy Clin Immunol*. 2015;135(1):273–275.
23. Salo PM, et al. Prevalence of allergic sensitization in the United States: results from the National Health and Nutrition Examination Survey (NHANES) 2005-2006. *J Allergy Clin Immunol*. 2014;134(2):350–359.
24. McGowan EC, Keet CA. Prevalence of self-reported food allergy in the National Health and Nutrition Examination Survey (NHANES) 2007-2010. *J Allergy Clin Immunol*. 2013;132(5):1216–1219.e5.
25. Eigenmann PA, Sicherer SH, Borkowski TA, Cohen BA, Sampson HA. Prevalence of IgE-mediated food allergy among children with atopic dermatitis. *Pediatrics*. 1998;101(3):E8.
26. Snapper SB, et al. Wiskott-Aldrich syndrome protein-deficient mice reveal a role for WASP in T but not B cell activation. *Immunity*. 1998;9(1):81–91.
27. Nguyen DD, et al. Lymphocyte-dependent and Th2 cytokine-associated colitis in mice deficient in Wiskott-Aldrich syndrome protein. *Gastroenterology*. 2007;133(4):1188–1197.
28. Föger N, Jenckel A, Orinska Z, Lee KH, Chan AC, Bulfone-Paus S. Differential regulation of mast cell degranulation versus cytokine secretion by the actin regulatory proteins Coronin1a and Coronin1b. *J Exp Med*. 2011;208(9):1777–1787.
29. Burton OT, et al. Oral immunotherapy induces IgG antibodies that act through FcγRIIb to suppress IgE-mediated hypersensitivity. *J Allergy Clin Immunol*. 2014;134(6):1310–1317.e6.
30. Hogan SP, Wang YH, Strait R, Finkelman FD. Food-induced anaphylaxis: mast cells as modulators of anaphylactic severity. *Semin Immunopathol*. 2012;34(5):643–653.

31. Caffarelli C, Romanini E, Caruana P, Street ME, de' Angelis G. Clinical food hypersensitivity: the relevance of duodenal immunoglobulin E-positive cells. *Pediatr Res*. 1998;44(4):485–490.

32. Brandt EB, et al. Mast cells are required for experimental oral allergen-induced diarrhea. *J Clin Invest*. 2003;112(11):1666–1677.

33. Burton OT, et al. Direct effects of IL-4 on mast cells drive their intestinal expansion and increase susceptibility to anaphylaxis in a murine model of food allergy. *Mucosal Immunol*. 2013;6(4):740–750.

34. Platzer B, et al. Dendritic cell-bound IgE functions to restrain allergic inflammation at mucosal sites. *Mucosal Immunol*. 2015;8(3):516–532.

35. Khodoun MV, Strait R, Armstrong L, Yanase N, Finkelman FD. Identification of markers that distinguish IgE- from IgG-mediated anaphylaxis. *Proc Natl Acad Sci U S A*. 2011;108(30):12413–12418.

36. Stefka AT, et al. Commensal bacteria protect against food allergen sensitization. *Proc Natl Acad Sci U S A*. 2014;111(36):13145–13150.

37. Noval Rivas M, et al. A microbiota signature associated with experimental food allergy promotes allergic sensitization and anaphylaxis. *J Allergy Clin Immunol*. 2013;131(1):201–212.

38. Cahenzli J, Köller Y, Wyss M, Geuking MB, McCoy KD. Intestinal microbial diversity during early-life colonization shapes long-term IgE levels. *Cell Host Microbe*. 2013;14(5):559–570.

39. Maillard MH, et al. The Wiskott-Aldrich syndrome protein is required for the function of CD4(+)CD25(+)Foxp3(+) regulatory T cells. *J Exp Med*. 2007;204(2):381–391.

40. Westerberg L, Larsson M, Hardy SJ, Fernández C, Thrasher AJ, Severinson E. Wiskott-Aldrich syndrome protein deficiency leads to reduced B-cell adhesion, migration, and homing, and a delayed humoral immune response. *Blood*. 2005;105(3):1144–1152.

41. Humblet-Baron S, et al. Wiskott-Aldrich syndrome protein is required for regulatory T cell homeostasis. *J Clin Invest*. 2007;117(2):407–418.

42. Marangoni F, et al. WASP regulates suppressor activity of human and murine CD4(+)CD25(+)FOXP3(+) natural regulatory T cells. *J Exp Med*. 2007;204(2):369–380.

43. Weiss JM, et al. Neuropilin 1 is expressed on thymus-derived natural regulatory T cells, but not mucosa-generated induced Foxp3+ T reg cells. *J Exp Med*. 2012;209(10):1723–1742.

44. Yadav M, et al. Neuropilin-1 distinguishes natural and inducible regulatory T cells among regulatory T cell subsets in vivo. *J Exp Med*. 2012;209(10):1713–1722.

45. Nurieva RI, et al. Transcriptional regulation of th2 differentiation by inducible costimulator. *Immunity*. 2003;18(6):801–811.

46. Tindemans I, Serafini N, Di Santo JP, Hendriks RW. GATA-3 function in innate and adaptive immunity. *Immunity*. 2014;41(2):191–206.

47. Noval Rivas M, et al. Regulatory T cell reprogramming toward a Th2-cell-like lineage impairs oral tolerance and promotes food allergy. *Immunity*. 2015;42(3):512–523.

48. Ulges A, et al. Protein kinase CK2 enables regulatory T cells to suppress excessive TH2 responses in vivo. *Nat Immunol*. 2015;16(3):267–275.

49. Matalon O, Reicher B, Barda-Saad M. Wiskott-Aldrich syndrome protein--dynamic regulation of actin homeostasis: from activation through function and signal termination in T lymphocytes. *Immunol Rev*. 2013;256(1):10–29.

50. Massaad MJ, Ramesh N, Geha RS. Wiskott-Aldrich syndrome: a comprehensive review. *Ann N Y Acad Sci*. 2013;1285:26–43.

51. Sicherer SH, Sampson HA. Food allergy. *J Allergy Clin Immunol*. 2010;125(2 Suppl 2):S116–S125.

52. Wang J, Sampson HA. Food allergy. *J Clin Invest*. 2011;121(3):827–835.

53. Recher M, et al. B cell-intrinsic deficiency of the Wiskott-Aldrich syndrome protein (WASp) causes severe abnormalities of the peripheral B-cell compartment in mice. *Blood*. 2012;119(12):2819–2828.

54. Morales-Tirado V, et al. Critical requirement for the Wiskott-Aldrich syndrome protein in Th2 effector function. *Blood*. 2010;115(17):3498–3507.

55. Pivniouk VI, et al. Impaired signaling via the high-affinity IgE receptor in Wiskott-Aldrich syndrome protein-deficient mast cells. *Int Immunol*. 2003;15(12):1431–1440.

56. Sommers CL, et al. A LAT mutation that inhibits T cell development yet induces lymphoproliferation. *Science*. 2002;296(5575):2040–2043.

57. Aguado E, et al. Induction of T helper type 2 immunity by a point mutation in the LAT adaptor. *Science*. 2002;296(5575):2036–2040.

58. Barda-Saad M, Braiman A, Titerence R, Bunnell SC, Barr VA, Samelson LE. Dynamic molecular interactions linking the T cell antigen receptor to the actin cytoskeleton. *Nat Immunol*. 2005;6(1):80–89.

59. Zhang J, et al. Antigen receptor-induced activation and cytoskeletal rearrangement are impaired in Wiskott-Aldrich syndrome protein-deficient lymphocytes. *J Exp Med*. 1999;190(9):1329–1342.

60. Vahl JC, et al. Continuous T cell receptor signals maintain a functional regulatory T cell pool. *Immunity*. 2014;41(5):722–736.

61. Levine AG, Arvey A, Jin W, Rudensky AY. Continuous requirement for the TCR in regulatory T cell function. *Nat Immunol*. 2014;15(11):1070–1078.

62. Wada T, et al. Somatic mosaicism in Wiskott-Aldrich syndrome suggests in vivo reversion by a DNA slippage mechanism. *Proc Natl Acad Sci U S A*. 2001;98(15):8697–8702.

63. Milner JD, et al. Early-onset lymphoproliferation and autoimmunity caused by germline STAT3 gain-of-function mutations. *Blood*. 2015;125(4):591–599.